

See discussions, stats, and author profiles for this publication at: <https://www.researchgate.net/publication/254394644>

The crystal structure of nanpingite-2M₂, the Cs end-member of muscovite

Article in *American Mineralogist* · February 1996

DOI: 10.2138/am-1996-1-213

CITATIONS

27

READS

32

2 authors, including:



John M. Hughes

University of Vermont

163 PUBLICATIONS 4,128 CITATIONS

SEE PROFILE

Some of the authors of this publication are also working on these related projects:



Tourmaline: petrology, trace element geochemistry, isotope geochemistry, geochronology, crystallography, crystal chemistry, provenance, etc... [View project](#)



polyoxometalate minerals [View project](#)

The crystal structure of nanpingite- $2M_2$, the Cs end-member of muscovite

YUNXIANG NI AND JOHN M. HUGHES

Department of Geology, Miami University, Oxford, Ohio 45056, U.S.A.

ABSTRACT

Nanpingite, ideally $\text{CsAl}_2(\text{AlSi}_3)\text{O}_{10}(\text{OH})_2$, is a Cs end-member dioctahedral mica, crystallizing in $C2/c$, with $a = 9.076(3)$, $b = 5.226(2)$, $c = 21.41(5)$ Å, and $\beta = 99.48(6)^\circ$. The crystal structure of type nanpingite was refined to $R = 0.058$ using single-crystal X-ray diffraction methods. Nanpingite is a $2M_2$ polytype dioctahedral mica rather than a $2M_1$ polytype as reported originally.

In comparison with the interlayer cations in common muscovite and paragonite, Cs^+ in nanpingite increases the [001] interlayer separation between adjacent 2:1 layers but has little effect on the lateral (a , b) cell dimensions. The existence of the rare $2M_2$ polytype is attributed to this large interlayer separation, which minimizes the repulsion of the superimposed (along [001]) O anions in the basal planes of neighboring tetrahedral layers. The $2M_2$ polytype involves ditrigonal prismatic coordination of the interlayer Cs^+ , in contrast to the octahedral coordination of interlayer K^+ and Na^+ in muscovite- $2M_1$ and paragonite- $2M_1$. The tetrahedral rotation in nanpingite is the smallest among dioctahedral micas and is also caused by the incorporation of the large interlayer cation Cs^+ .

INTRODUCTION

Nanpingite is a 2:1 dioctahedral mica, similar in composition to muscovite but with Cs^+ as the interlayer cation. The mineral (Yang et al. 1988) results from the late-stage evolution of a large granitic pegmatite in the Nanping pegmatite field, Fujian, China. Nanpingite occurs in the center of the large pegmatite vein that crystallized from a residual hydrothermal fluid with very high Cs content; no other occurrence is known to date.

The crystal structures of dioctahedral micas and their polytypism have been extensively studied and reported, as have the crystallographic effects of the interlayer cation size on polytype and tetrahedral rotation. Bailey (1984) provided an excellent review of the crystal chemistry of dioctahedral micas. Takeda and Burnham (1969) and Takeda et al. (1971) specifically discussed the stability of the $2M_2$ polytype. Guggenheim (1981) reviewed previous work on the variation in coordination of the interlayer cation for the $2M_2$ polytype vs. other polytypes in lepidolite. In nanpingite, the largest interlayer cation, Cs^+ , is an additional data point to consider in further delineating how the size of the interlayer cation affects the mica structure ($^{133}\text{Cs}^+$, 1.88 Å, compared with $^{41}\text{K}^+$, 1.64 Å; radii from Shannon 1976). An additional advantage of this nanpingite study is that comparison can be made with other micas with essentially identical octahedral sheets, so that the effect of only the interlayer cation substituent can be observed.

EXPERIMENTAL METHODS

Crystals of nanpingite were hand-picked from crushed material from the type specimens (Yang et al. 1988) from

the Nanping pegmatite. The samples examined for X-ray study were from the same separate as the type specimens used by Yang et al. (1988) in their description of the mineral. Tens of crystals were examined by precession photography, and virtually all were found to exhibit streaking of the diffractions from bent crystallites caused by the trimming of crystals, as the mineral is more ductile than common micas. A single crystal that displayed essentially no streaking of spots was isolated. The crystal measured $0.26 \times 0.22 \times 0.03$ mm.

Before the structure refinement, the polytype of nanpingite was determined by examination of a complete set of precession photographs, which were compared with the typical precession photos given by Bailey (1988). The current study indicates that the true polytype is $2M_2$ rather than $2M_1$ as originally reported (Yang et al. 1988).

Examination of the photographs revealed that the extinction rules for nanpingite are $(0k0)$ $k = 2n$, $(h0l)$ $h + l = 2n$, and (hkl) $h + k = 2n$. Thus, one of the pseudo-hexagonal a axes is a diad perpendicular to a c -glide plane, yielding space groups Cc or $C2/c$, the latter of which is the space group of muscovite. The structure refinement proceeded routinely in space group $C2/c$ using the crystal-structure model of phengite- $2M_2$ given by Zhoukhlistov et al. (1973).

X-ray intensity data for nanpingite were collected on an Enraf-Nonius CAD-4 diffractometer utilizing graphite-monochromated $\text{MoK}\alpha$ radiation for the hemisphere of reciprocal space encompassing $k > 0$. Unit-cell parameters were refined (no symmetry constraints) using diffraction angles from 25 automatically centered reflections. Crystal data are given in Table 1, which records details of data collection and structure refinement.

TABLE 1. Crystal data and results of structure refinements for nanpingite

Dimensions (mm)	0.26 × 0.22 × 0.03
Unit cell	
Least squares	
<i>a</i> (Å)	9.076(3)
<i>b</i> (Å)	5.226(2)
<i>c</i> (Å)	21.41(5)
α (°)	89.97(7)
β (°)	99.48(6)
γ (°)	89.97(3)
Constrained (space group: $C2/c$)	
<i>a</i> (Å)	9.0756
<i>b</i> (Å)	5.2263
<i>c</i> (Å)	21.4088
β (°)	99.4820
θ limits	0.05–30°
Standards	
Intensity	3 per 4 h
Orientation	3 per 250 refl.
Data collected	2937
Unique data	1471
Data > $3\sigma_I$	680
Scan type	$\theta/2\theta$
Scan time (s)	≤70
R_{merge}	0.040
R	0.058
R_w	0.076
Goodness of fit	1.307
Variables	89
Largest peaks on difference map (e/Å ³)	
(+)	2.660
(-)	1.369

Note: Numbers in parentheses denote one estimated standard deviation of last digit cited. Chemical composition ($Z = 4$), cited from Yang et al. (1988), is $(\text{Cs}_{0.88}\text{K}_{0.06}\text{Rb}_{0.01})_{0.95}(\text{Al}_{1.64}\text{Mg}_{0.22}\text{Fe}_{0.17}\text{Li}_{0.15}\text{Zr}_{0.16})[\text{Si}_{3.16}\text{Al}_{0.84}\text{O}_{10}][(\text{OH})_{1.79}\text{F}_{0.21}]_2$.

The SDP package of computer programs (Frenz 1985) was used to solve and refine the structure. Intensity data were reduced to structure factors and corrected for Lorentz and polarization effects. Absorption effects were initially corrected using $360^\circ \psi$ -scan data for nine reflections; after attaining solution, we also employed absorption corrections using the absorption-surface method implemented in the program Difabs (Walker and Stuart 1983). Symmetry-equivalent reflections were averaged (Table 1), and neutral-atom scattering factors with terms for anomalous dispersion were used. Reflections were weighted proportional to σ^{-2} , and reflections with $I > 3\sigma_I$ were used in the refinement. The chemical formula of the type material is also given in Table 1.

The powder X-ray diffraction pattern of nanpingite- $2M_2$ was measured on a Scintag X1 diffractometer. The peaks were profile-fitted, and all were successfully indexed on the basis of the $2M_2$ polytype structure. The unit cell was also refined using the observed powder diffraction pattern, yielding $a = 9.087(2)$, $b = 5.230(1)$, $c = 21.519(5)$ Å, $\beta = 99.48(2)^\circ$, which is comparable to the unit cell refined by the single-crystal technique as in Table 1. Table 2 lists the observed and calculated diffraction patterns of nanpingite. The program POWD10 (Smith et al. 1983) was used to calculate the pattern from the refined crystal structure.

Table 3 contains positional parameters and equivalent isotropic thermal parameters, and Table 4 contains selected bond lengths for nanpingite. Table 5 presents anisotropic displacement parameters, and Table 6 lists observed and calculated structure factors.¹ The bond-valence sums of all atoms in nanpingite were calculated using the method and constants of Brown (1981) and are in good agreement with the formal valence of the atoms. The bond-valence sum of O6 (0.96 valence units) indicates that O6 is an OH group; no attempt was made to locate or refine the H atom.

DESCRIPTION OF THE NANPINGITE ATOMIC ARRANGEMENT

Like muscovite, nanpingite is a dioctahedral mica; it consists of 2:1 layers separated by interlayer Cs^+ ions. Unlike most dioctahedral micas, however, nanpingite is a $2M_2$ polytype; the 2:1 layers in nanpingite are stacked by rotating adjacent layers 60 or 180° rather than 0 or 120° as in $2M_1$ muscovite. As a result, two neighboring octahedral sheets in nanpingite are different "sets" (sets I and II, defined in Bailey 1984) or site occupancies, whereas in $2M_1$ muscovite they are the same set. Because the $2M_2$ polytype is rare in dioctahedral micas, this property of nanpingite is of special interest.

The incorporation of Cs^+ as the interlayer cation has predictable effects on the unit cell of nanpingite (Table 1). The Cs^+ polyhedron is enlarged along c^* relative to the K^+ polyhedron in muscovite, but it is not enlarged in (001) because the rigid octahedral sheets control cell dimension in that plane.

Figure 1 presents the relationships between the average radius of univalent interlayer cations and unit-cell parameters in dioctahedral micas. Unit-cell thickness ($c \sin \beta$) increases with increasing cation size, whereas a and b (note that the $2M_2$ polytype has reversed values for a and b relative to the $2M_1$ polytype) increase little because of the rigidity of the octahedral sheet. The increase of ($c \sin \beta$) values results from the increase in size of the interlayer cation; however, the relationship is not linear, as the interlayer distance increases by an amount greater than the increase in the diameter of the interlayer cation (Fig. 2). For example, the difference between the interlayer separations of paragonite (Lin and Bailey 1984) and nanpingite is 0.944 Å, but the difference between the average diameters of the cations is only 0.92 Å (Shannon 1976); the difference between the interlayer separations of muscovite (Rothbauer 1971) and nanpingite is 0.60 Å, whereas the difference in the average diameters is 0.48 Å (Shannon 1976).

This disparity between the interlayer separations predicted by cation radius and the actual separation is at-

¹ A copy of Tables 5 and 6 may be ordered as Document AM-96-605 from the Business Office, Mineralogical Society of America, 1015 Eighteenth Street NW, Suite 601, Washington, DC 20036, U.S.A. Please remit \$5.00 in advance for the microfiche.

TABLE 2. X-ray diffraction patterns of nanpingite-2M₂ calculated from the crystal structure and measured by powder diffractometry

<i>hkl</i>	<i>d</i> _{calc} (Å)	<i>l</i> / <i>l</i> ₀	<i>d</i> _{obs} (Å)	<i>l</i> / <i>l</i> ₀	<i>hkl</i>	<i>d</i> _{calc} (Å)	<i>l</i> / <i>l</i> ₀	<i>d</i> _{obs} (Å)	<i>l</i> / <i>l</i> ₀
002	10.56	5	10.61	13	221	2.264	20	2.267	8
004	5.279	2	5.300	11	220	2.257	5	2.256	4
110	4.513	6	4.515	3	316	2.246	11	2.247	6
200	4.476	26	4.483	13	400	2.238	12	2.236	5
202	4.389	2	4.387	2	221	2.224	18	2.227	10
111	4.341	40	4.347	21	314	2.205	14	2.208	11
112	4.280	27	4.289	12	317	2.121	20	2.133	7
112	4.031	49	4.041	25	0,0,10	2.112	24	2.123	74
113	3.951	62	3.961	36	026	2.098	12	2.103	4
202	3.897	28	3.903	17	315	2.080	18	2.085	6
204	3.731	98	3.740	55	406	2.047	5	2.054	2
113	3.664	20	3.674	9	318	1.998	7	2.004	2
114	3.581	100	3.591	65	1,1,10	1.977	2	1.983	4
114	3.298	83	3.308	63	316	1.957	8	1.962	2
115	3.220	18	3.231	11	1,1,10	1.855	4	1.863	3
204	3.167	71	3.176	51	1,1,11	1.822	4	1.831	3
206	3.019	29	3.029	22	2,0,10	1.799	2	1.807	2
115	2.963	39	2.974	30	3,1,10	1.765	16	1.771	5
116	2.894	42	2.904	31	029	1.746	15	1.751	6
116	2.670	18	2.675	16	318	1.730	12	1.736	4
008	2.640	34	2.653	100	510	1.694	3	1.696	3
312	2.604	47	2.608	18	421	1.678	7	1.681	3
021	2.593	54	2.597	20	511	1.668	4	1.667	3
313	2.553	8	2.560	2	425	1.650	12	1.652	3
022	2.536	3	2.541	2	516	1.629	11	1.632	4
311	2.529	6	2.530	2	135	1.603	12	1.605	4
208	2.458	6	2.469	6	135	1.568	5	1.569	3
118	2.366	5	2.376	5					

tributed to the coordination for which the cation radii are selected. The radii discussed above are based on a coordination number of 12 for the interlayer cations. However, unlike the more regular bonds to the interlayer cation in nanpingite, in paragonite and muscovite the bonds (distances) to Na⁺ and K⁺, respectively, can be considered as two distinct groups, six inner bonds and six outer distances [this is not a new concept and has been reviewed by Guggenheim (1981) and Bailey (1984)]. As noted in Figure 2, the outer distances are independent of the radius of the interlayer cation, whereas the inner bonds increase in length with increasing radius of the interlayer cation. The differences between the bond lengths vary inversely with interlayer spacing; in paragonite the inner and outer distances differ by 0.746 Å (Lin and Bailey 1984), whereas in muscovite the inner and outer bonds differ by 0.505 Å (Rothbauer 1971). In nanpingite, however, the difference between the two sets of bonds is 0.239 Å, the smallest among dioctahedral micas. The coordination polyhedron of the interlayer cation in nanpingite also differs from that in paragonite and muscovite. In nanpingite-2M₂, the Cs⁺ atom is coordinated by 12 O atoms in a ditrigonal prism, whereas in the 2M₁ phases muscovite and paragonite the interlayer cations have six nearest neighbors in the form of an octahedron.

As expected, because of the rigidity of the octahedral sheets, the lateral (*a*, *b*) dimensions in nanpingite are similar to those of other dioctahedral micas. The lateral edges of octahedra in nanpingite, as in muscovite, display a shorter shared edge and a longer unshared edge resulting from the vacant M1 polyhedron (Table 4). As a result of

this distortion, the octahedral sheet is flattened to 2.079 Å. It is well known that the distortion and enlargement of the tetrahedral sheet that result from the substitution of Al for Si induce a misfit between the octahedral and tetrahedral sheets. To relieve this misfit, adjacent tetrahedra rotate in opposite directions in (001), thus changing the shape of the tetrahedral ring from hexagonal to ditrigonal. In addition, the tetrahedral sheet is thickened to 2.241 Å in nanpingite. The tetrahedral rotation, octahedral flattening, and tetrahedral thickening are expressed by the indices α , ψ , and τ (Donnay et al. 1964). In nanpingite, $\alpha = 5.45$, $\psi_{M1} = 62.40$, $\psi_{M2} = 57.58$ ($\psi_{ideal} = 54.73$), $\tau_{T1} = 111.4$, and $\tau_{T2} = 111.4^\circ$ ($\tau_{ideal} = 109.47^\circ$). It is noteworthy that the tetrahedral rotation angle, α , in

TABLE 3. Atomic coordinates and isotropic *B* value for atoms in nanpingite

Atom	Site	<i>x</i>	<i>y</i>	<i>z</i>	<i>B</i> (Å ²)*
Cs	4e	0	0.0961(2)	¼	1.83(2)
M1	4d	¾	¼	0	
M2	8f	0.0837(3)	0.2503(6)	0.0000(2)	0.91(6)
T1	8f	0.1197(3)	0.5884(6)	0.1272(2)	1.09(5)
T2	8f	0.2901(3)	0.1009(6)	0.1271(2)	1.09(5)
O1	8f	0.0763(7)	0.561(1)	0.0505(4)	1.6(2)
O2	8f	0.2672(8)	0.132(1)	0.0504(4)	1.5(2)
O3	8f	0.2053(8)	0.332(1)	0.1581(4)	1.3(2)
O4	8f	0.4670(7)	0.121(2)	0.1591(4)	1.5(2)
O5	8f	0.2319(9)	0.825(2)	0.1489(5)	1.9(2)
O6 (=OH)	8f	0.9545(8)	0.062(2)	0.0468(4)	1.5(2)

Note: Numbers in parentheses denote one estimated standard deviation of last digit cited.

* Equivalent isotropic *B* value calculated from refined anisotropic parameters.

TABLE 4. Selected interatomic distances and angles in nanpingite

Atomic distances (Å)			Angles (°)		
Cs ditrigonal prism			Edge of ditrigonal prism		
	inner	outer		larger	smaller
Cs-O3 × 2	3.174(9)	3.345(7)	O3-O4-O5	131.2(4)	108.7(4)
Cs-O4 × 2	3.141(8)	3.347(8)	O3-O5-O4	131.7(4)	107.2(4)
Cs-O5 × 2	3.209(8)	3.55(1)	O4-O3-O5	130.6(4)	108.9(4)
Mean	3.175	3.414	Mean	131.2	108.3
T1 tetrahedron					
T1-O1	1.64(1)				
T1-O3	1.631(9)				
T1-O4	1.651(8)				
T1-O5	1.620(9)				
Mean	1.636				
O1-O3	2.69(1)	O1-T1-O3	110.9(5)		
O1-O4	2.69(1)	O1-T1-O4	110.2(4)		
O1-O5	2.71(1)	O1-T1-O5	113.1(5)		
O3-O4	2.64(1)	O3-T1-O4	107.0(5)		
O3-O5	2.60(1)	O3-T1-O5	109.5(5)		
O4-O5	2.67(1)	O4-T1-O5	109.5(5)		
Mean	2.67	Mean	109.4		
T2 tetrahedron					
T2-O2	1.63(1)				
T2-O3	1.633(9)	T1-O3-T2	132.0(6)		
T2-O4	1.641(7)	T1-O4-T2	130.7(6)		
T2-O5	1.631(9)	T1-O5-T2	144.2(6)		
Mean	1.634	Mean	135.6		
O2-O3	2.68(1)	O2-T2-O3	110.3(4)		
O2-O4	2.70(1)	O2-T2-O4	111.5(4)		
O2-O5	2.71(1)	O2-T2-O5	112.5(5)		
O3-O4	2.62(1)	O3-T2-O4	106.2(4)		
O3-O5	2.67(1)	O3-T2-O5	110.1(5)		
O4-O5	2.62(1)	O4-T2-O5	106.1(4)		
Mean	2.67	Mean	109.5		
M1 octahedron (vacant)					
M1-O1 × 2	2.278				
M1-O2 × 2	2.262				
M1-OH × 2	2.191				
Mean	2.244				
O1-O2 × 2	3.451	O1-M1-O2 × 2	98.92		
O1-OH × 2	3.446	O1-M1-OH × 2	100.88		
O2-OH × 2	3.437	O2-M1-OH × 2	101.01		
Mean (unshared)	3.445	Mean (unshared)	100.27		
O1-O2	2.952	O1-M1-O2	81.08		
O1-OH	2.847	O1-M1-OH	79.12		
O2-OH	2.883	O2-M1-OH	78.99		
Mean (shared)	2.894	Mean (shared)	79.73		
M2 octahedron					
M2-O1	1.959(9)				
M2-O1	1.931(8)				
M2-O2	1.932(8)				
M2-O2	1.964(9)				
M2-OH	1.933(9)				
M2-OH	1.916(9)				
Mean	1.939				
O1-O2	2.84(1)	O1-M2-O2	93.6(4)		
O1-O2	2.83(1)	O1-M2-O2	93.1(4)		
O1-OH	2.83(1)	O1-M2-OH	93.3(4)		
O1-OH	2.85(1)	O1-M2-OH	94.9(3)		
O2-OH	2.83(1)	O2-M2-OH	95.0(4)		
O2-OH	2.83(1)	O2-M2-OH	93.6(4)		
Mean (unshared)	2.83	Mean (unshared)	93.9		
O1-O1	2.45(1)	O1-M2-O1	78.2(4)		
O2-O2	2.46(1)	O2-M2-O2	78.5(4)		
OH-OH	2.38(1)	OH-M2-OH	76.4(4)		
Mean (shared)	2.43	Mean (shared)	77.7		

Note: Numbers in parentheses denote one estimated standard deviation of last digit cited.

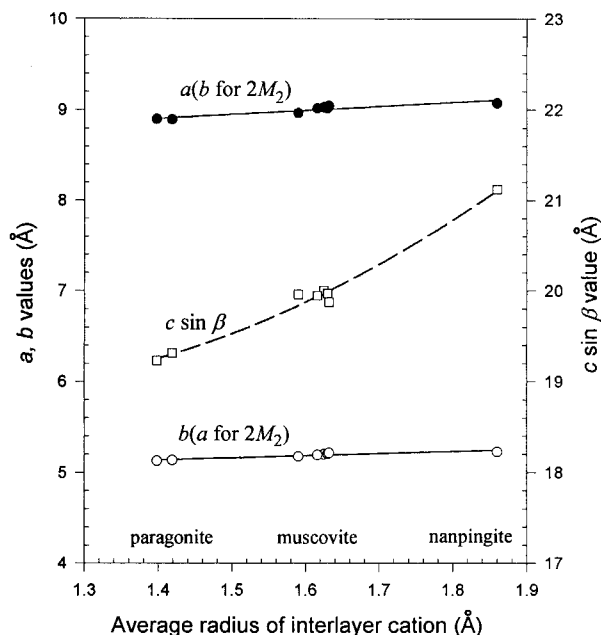


FIGURE 1. Variation of unit-cell parameters with average radius in selected 2:1 dioctahedral micas. Data for paragonite and muscovite are from Lin and Bailey (1984), Richardson and Richardson (1982), Knurr and Bailey (1986), Rule and Bailey (1985), Rothbauer (1971), Sidorenko et al. (1977), and Zhoukhlistov et al. (1973).

nanpingite is the smallest value found in any dioctahedral mica (6–19°, Bailey 1984).

DISCUSSION OF THE STRUCTURE AND POLYTYPE

There are two distinct features of the nanpingite crystal structure. First, nanpingite is rare among dioctahedral micas in that it crystallizes as a $2M_2$ polytype. Second, nanpingite exhibits a tetrahedral rotation angle, α , that is uniquely small among dioctahedral micas. Both features are attributed to the large Cs^+ cation. The original X-ray diffraction study of nanpingite (Yang et al. 1988) emphasized the parallelism between nanpingite and muscovite, except for the different interlayer cations. Those authors thus assumed that nanpingite is a $2M_1$ mica polytype, the most common polytype among dioctahedral micas; this assumption also persisted in the publication of PDF card no. 44-1428. The current study indicates that the true polytype is $2M_2$, a rare polytype among dioctahedral micas. The reasons for the existence of this polytype become clear upon examination of the atomic arrangement.

One dioctahedral phengite was reported to crystallize as a $2M_2$ polytype (Zhoukhlistov et al. 1973) on the basis of an electron diffraction study. Zhoukhlistov et al. (1973) suggested that the substitution of relatively few Al^{3+} for Si^{4+} atoms balances the charge in the basal O-atom surface of the tetrahedral sheet, causing less interlayer repulsion, thereby producing conditions for a $2M_2$ polytype to crystallize. The removal of the repulsion between the

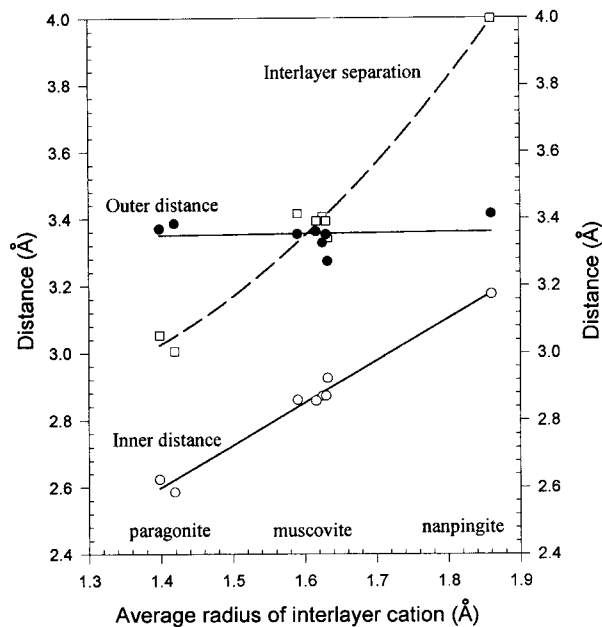


FIGURE 2. Bond lengths of inner and outer bonds of interlayer cation polyhedron and interlayer separation vs. average radius of interlayer cation in selected 2:1 dioctahedral micas. Sources of paragonite and muscovite data are the same as in Figure 1.

basal O-atom planes of adjacent 2:1 layers is thus critical in the determination of polytype, as the stacking sequence in the $2M_2$ polytype yields an atomic arrangement "in which three basal oxygens from one layer directly superimpose on three basal oxygens from the layer below" (Bailey 1984, p. 34), and is thus energetically unfavorable relative to the $2M_1$ polytype. In nanpingite, the unfavorable repulsion between adjacent basal O-atom planes is mitigated by the increased interlayer separation that results from the incorporation of the large interlayer cation Cs^+ and not by reduction of the net charge on the basal O atoms. The distance between adjacent basal O-atom layers in nanpingite is 3.997 Å, in comparison with ~3.4 Å in muscovite and ~3.05 Å in paragonite. The repulsion between the layers is thus minimized, allowing ditrigonal prismatic coordination of the Cs^+ ion and [001] superposition of basal O atoms that results in a $2M_2$ polytype (Fig. 3).

The second distinct feature of nanpingite is the exceptionally small α angle. As illustrated in Figure 3, the hexagonal tetrahedral ring is nearly ideal, displaying only a small deviation from the ideal 120° O-O-O angle. This feature is also attributed to the incorporation of the large interlayer cation. As noted by Bailey (1984), the space available for the interlayer cation is reduced with increasing distortion (α). Hewitt and Wones (1975), in an analysis of a series of synthetic and natural micas, concluded that the observed tetrahedral rotations in the dioctahedral micas muscovite and paragonite indicate that the size of the interlayer cation in part controls the amount

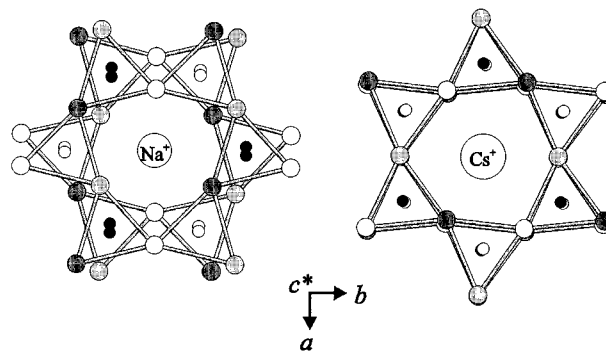


FIGURE 3. Environments of interlayer cations in nanpingite- $2M_2$ (right) and paragonite- $2M_1$ (left), projected on (001). Small open circles = T1, small solid circles = T2, larger open circles = O3, lightly shaded larger circles = O4, and densely shaded larger circles = O5.

of tetrahedral rotation in the structure. They demonstrated that larger interlayer cations inhibit larger α rotations because such rotations decrease the size of the interlayer cation site. The Cs^+ interlayer cation in nanpingite requires the largest cation site among dioctahedral micas, which increases the inner distances because the outer distances are independent of the cations (Fig. 2). The minimized difference between the inner and outer distances keeps the tetrahedral rotation to a minimum in the phase.

Finally, it is noted that from the chemical formula (Table 1), light elements such as Li^+ may occupy up to 15% of the vacant M1 position. However, the relatively high R value of this refinement does not allow us to locate any excessive electron density at that site; the electron density at the M1 position is $<0.554 \text{ e}/\text{\AA}^3$.

ACKNOWLEDGMENTS

Special thanks are due to S. Guggenheim for reviewing the manuscript and contributing many important insights to the study. R.A. Eggleton also provided an insightful review of the manuscript. Support for this study was provided by the U.S. National Science Foundation through grants EAR-9218577 and EAR-9403194 (to J.M.H.).

REFERENCES CITED

- Bailey, S.W. (1984) Crystal chemistry of the true micas. In *Mineralogical Society of America Reviews in Mineralogy*, 13, 13–60.
- (1988) X-ray diffraction identification of the polytypes of mica, serpentine and chlorite. *Clays and Clay Minerals*, 36, 193–213.
- Brown, I.D. (1981) The bond-valence method: An empirical approach to chemical structure and bonding. In M. O'Keeffe and A. Navrotsky, Eds., *Structure and bonding in crystals*, volume 2, p. 1–30. Academic, New York.
- Donnay, G., Donnay, J.D.H., and Takeda, H. (1964) Trioctahedral one-layer micas: II. Prediction of the structure from composition and cell dimensions. *Acta Crystallographica*, 17, 1374–1381.
- Frenz, B.A. (1985) Enraf-Nonius structure determination package. In *SDP Users Guide*, version 4. Enraf-Nonius, Delft, the Netherlands.
- Guggenheim, S. (1981) Cation ordering in lepidolite. *American Mineralogist*, 66, 1221–1232.
- Hewitt, D.A., and Wones, D.R. (1975) Physical properties of some synthetic Fe-Mg-Al trioctahedral biotites. *American Mineralogist*, 60, 854–862.

- Knurr, R.A., and Bailey, S.W. (1986) Refinement of Mn-substituted muscovite and phlogopite. *Clays and Clay Minerals*, 34, 7–16.
- Lin, C.-Y., and Bailey, S.W. (1984) The crystal structure of paragonite- $2M_1$. *American Mineralogist*, 69, 122–127.
- Richardson, S.M., and Richardson, J.W., Jr. (1982) Crystal structure of a pink muscovite from Archer's Post, Kenya: Implications for reverse pleochroism in dioctahedral micas. *American Mineralogist*, 67, 69–75.
- Rothbauer, R. (1971) Untersuchung eines $2M_1$ -Muskovits mit Neutronenstrahlen. *Neues Jahrbuch für Mineralogie Monatshefte*, 143–154.
- Rule, A.C., and Bailey, S.W. (1985) Refinement of the crystal structure of phengite- $2M_1$. *Clays and Clay Minerals*, 33, 403–409.
- Shannon, R.D. (1976) Revised effective ionic radii and systematic studies of interatomic distances in halides and chalcogenides. *Acta Crystallographica*, A32, 751–767.
- Sidorenko, O.V., Zvyagin, B.B., and Soboleva, S.V. (1977) Refinement of the crystal structure of $2M_1$ paragonite by the method of high-voltage electron diffraction. *Soviet Physics Crystallography*, 22, 554–556 (translated from *Kristallografiya*, 22, 971–975, 1977).
- Smith, D.K., Nichols, M.C. and Zolensky, M.E. (1983) POWD10, a Fortran IV program for calculating X-ray powder diffraction patterns. Pennsylvania State University, University Park.
- Takeda, H., and Burnham, C. W. (1969) Fluor-polyolithionite: a lithium mica with nearly hexagonal $(\text{Si}_2\text{O}_5)^{2-}$ ring. *Mineralogical Journal (Japan)*, 6, 102–109.
- Takeda, H., Haga, N., and Sadanaga, R. (1971) Structural investigation of polymorphic transition between $2M_2$ -, $1M$ -lepidolite and $2M_1$ muscovite. *Mineralogical Journal (Japan)*, 6, 203–215.
- Walker, N., and Stuart, D. (1983) An empirical method for correcting diffractometer data for absorption effects. *Acta Crystallographica*, A39, 158–166.
- Yang, Y., Ni, Y., Wang, L., and Wang W. (1988) Nanpingite: A new cesium mineral. *Acta Petrologica et Mineralogica (China)*, 7(1), 49–58.
- Zhoukhlistov, A.P., Zvyagin, B.B., Soboleva, S.V., and Fedotov, A.F. (1973) The crystal structure of the dioctahedral mica $2M_2$ determined by high voltage electron diffraction. *Clays and Clay Minerals*, 21, 465–470.

MANUSCRIPT RECEIVED NOVEMBER 21, 1994

MANUSCRIPT ACCEPTED SEPTEMBER 14, 1995